

This item is the archived peer-reviewed author-version of:

An adjoint method for the exact calibration of stochastic local volatility models

Reference:

Wyns Maarten, in 't Hout Karel.- An adjoint method for the exact calibration of stochastic local volatility models
Journal of Computational Science - ISSN 1877-7503 - 24(2018), p. 182-194
Full text (Publisher's DOI): <https://doi.org/10.1016/J.JOCS.2017.02.004>
To cite this reference: <https://hdl.handle.net/10067/1489720151162165141>

An adjoint method for the exact calibration of Stochastic Local Volatility models

Maarten Wyns* and Karel J. in 't Hout*

February 8, 2017

Abstract

This paper deals with the exact calibration of semidiscretized stochastic local volatility (SLV) models to their underlying semidiscretized local volatility (LV) models. Under an SLV model, it is common to approximate the fair value of European-style options by semidiscretizing the backward Kolmogorov equation using finite differences. In the present paper we introduce an adjoint semidiscretization of the corresponding forward Kolmogorov equation. This adjoint semidiscretization is used to obtain an expression for the leverage function in the pertinent SLV model such that the approximated fair values defined by the LV and SLV models are identical for non-path-dependent European-style options. In order to employ this expression, a large non-linear system of ODEs needs to be solved. The actual numerical calibration is performed by combining ADI time stepping with an inner iteration to handle the non-linearity. Ample numerical experiments are presented that illustrate the effectiveness of the calibration procedure.

Key words: Stochastic local volatility; Adjoint spatial discretization; Calibration; Finite differences; ADI methods.

1 Introduction

In contemporary financial mathematics, *stochastic local volatility (SLV) models* are state-of-the-art for describing asset price processes, notably foreign exchange (FX) rates, see e.g. [21, 29]. They constitute a natural combination of *local volatility (LV)* and *stochastic volatility (SV)* models. Denote by $S_\tau > 0$ the FX rate at time $\tau \geq 0$ and consider the standard transformed variable $X_\tau = \log(S_\tau/S_0)$. We deal in this paper with general SLV models of the type

$$\begin{cases} dX_\tau = (r_d - r_f - \frac{1}{2}\sigma_{SLV}^2(X_\tau, \tau)\psi^2(V_\tau))d\tau + \sigma_{SLV}(X_\tau, \tau)\psi(V_\tau)dW_\tau^{(1)}, \\ dV_\tau = \kappa(\eta - V_\tau)d\tau + \xi V_\tau^\alpha dW_\tau^{(2)}, \end{cases} \quad (1.1)$$

with $\psi(v)$ a non-negative function, α a non-negative parameter, κ, η, ξ strictly positive parameters, $dW_\tau^{(1)} \cdot dW_\tau^{(2)} = \rho d\tau$, $-1 \leq \rho \leq 1$, and given spot values S_0, V_0 . The function $\sigma_{SLV}(x, \tau)$ is often called *the leverage function* and r_d , respectively r_f , denotes the risk-free interest rate in the domestic currency, respectively foreign currency. The SLV model (1.1) can be viewed as obtained from a mixture of the LV model

$$dX_{LV,\tau} = (r_d - r_f - \frac{1}{2}\sigma_{LV}^2(X_{LV,\tau}, \tau))d\tau + \sigma_{LV}(X_{LV,\tau}, \tau)dW_\tau, \quad (1.2)$$

*Department of Mathematics and Computer Science, University of Antwerp, Middelheimlaan 1, B-2020 Antwerp, Belgium. Email: {maarten.wyns,karel.inthout}@uantwerpen.be.

with LV function $\sigma_{LV}(x, \tau)$, and the SV model

$$\begin{cases} dX_{SV,\tau} = (r_d - r_f - \psi^2(V_{SV,\tau}))d\tau + \psi(V_{SV,\tau})dW_\tau^{(1)}, \\ dV_{SV,\tau} = \kappa(\eta - V_{SV,\tau})d\tau + \xi V_{SV,\tau}^\alpha dW_\tau^{(2)}. \end{cases} \quad (1.3)$$

Clearly, if $\sigma_{SLV}(x, \tau)$ is identically equal to one, then the SLV model reduces to a SV model. Next, if the stochastic volatility parameter ξ is equal to zero, then the SLV model reduces to a LV model.

The choice $\psi(v) = \sqrt{v}$, $\alpha = 1/2$ corresponds to the well-known Heston-based S(L)V model, the choice $\psi(v) = v$, $\alpha = 1$ to the S(L)V model considered in [29] and the choice $\psi(v) = \exp(v)$, $\alpha = 0$ corresponds to the S(L)V model based on the exponential Ornstein–Uhlenbeck model described in [27].

If α is strictly positive, we assume that $\psi(0) = 0$ and the processes $V_\tau, V_{SV,\tau}$ are non-negative. For $0 < \alpha < 1/2$ it holds that $V_\tau = 0$ is attainable, for $\alpha > 1/2$ it holds that $V_\tau = 0$ is unattainable, and for $\alpha = 1/2$ one has that $V_\tau = 0$ is attainable if $2\kappa\eta < \xi^2$, see e.g. [1]. The analogous result is true for the pure SV model (1.3).

In financial practice, $\sigma_{LV}(x, \tau)$ is determined such that the LV model (1.2) yields the exact market prices for vanilla options, see e.g. [3, 6], and the parameters κ, η, ξ are chosen such that the SV model (1.3) reflects the market dynamics of the underlying asset, see e.g. [29]. Next, the leverage function σ_{SLV} is calibrated such that the SLV model yields the exact market prices for European call and put options. In the literature, no closed-form analytical relationship appears to be available between the leverage function and the fair value of vanilla options within the SLV model. Accordingly, in financial practice the leverage function is calibrated by making use of a relationship between the SLV model and the LV model. It is well-known, see e.g. [9, 28], that these models yield the same marginal distribution for the exchange rate S_τ , and hence always define the same fair value for vanilla options, if the leverage function $\sigma_{SLV}(x, \tau)$ satisfies

$$\sigma_{LV}^2(x, \tau) = \mathbb{E}[\sigma_{SLV}^2(X_\tau, \tau)\psi^2(V_\tau)|X_\tau = x] = \sigma_{SLV}^2(x, \tau)\mathbb{E}[\psi^2(V_\tau)|X_\tau = x], \quad (1.4)$$

for all $x \in \mathbb{R}, \tau \geq 0$. The latter conditional expectation can be written as

$$\mathbb{E}[\psi^2(V_\tau)|X_\tau = x] = \frac{\int_{-\infty}^{\infty} \psi^2(v)p(x, v, \tau; X_0, V_0)dv}{\int_{-\infty}^{\infty} p(x, v, \tau; X_0, V_0)dv}, \quad (1.5)$$

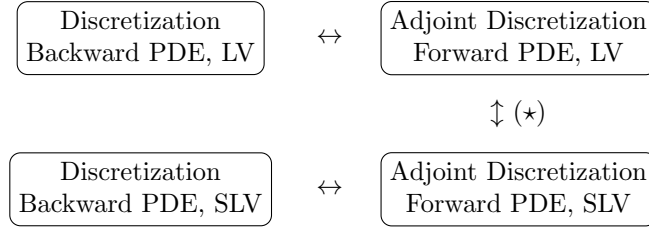
where $p(x, v, \tau; X_0, V_0)$ denotes the joint density of (X_τ, V_τ) given by the SLV model. Since the LV function is determined such that the LV model yields exactly the observed market prices for vanilla options, the SLV model will also exactly define the same fair value whenever one is able to determine the conditional expectation above and defines the leverage function by (1.4). This conditional expectation itself depends on $\sigma_{SLV}(x, \tau)$, however, and determining it is a highly non-trivial task. Recently, a variety of numerical techniques, see e.g. [4, 8, 11, 25, 31], has been proposed in order to approximate this conditional expectation and to approximate the appropriate leverage function.

The numerical techniques presented in the references above do not take into account explicitly that, even if the LV function is known analytically, it is often not possible to determine exactly the corresponding fair value of vanilla options. Even within the LV model one relies on numerical methods in order to approximate the fair option values. A common approach consists of numerically solving the corresponding backward partial differential equation (PDE) by for example finite difference or finite volume methods, see e.g. [30]. When calibrating the SLV model to the LV model, the best result one can thus aim for is that the numerical approximation of the fair value of vanilla options is the same for both models whenever similar numerical valuation methods are used.

In this paper we assume that the fair option value (within the LV model, resp. SLV model) is approximated through numerically solving the backward PDE (corresponding to the LV model, resp. SLV model) by standard finite difference or finite volume methods. Given such a spatial

discretization for the backward PDE, an *adjoint spatial discretization* will be introduced for the corresponding forward PDE. This adjoint spatial discretization has the important property that it always defines *exactly the same approximation* for the fair value of non-path-dependent European options as the approximation given by the discretization of the backward equation. Moreover, if similar spatial discretizations are used for the backward PDE associated with the LV model and the backward PDE associated with the SLV model, then their adjoint spatial discretizations can be employed to *create an exact match between the approximations for the fair value of vanilla options within the LV model and the SLV model*.

The main contributions of this article can be visualized in the following scheme:



Here relationship (\star) can only be achieved if similar discretizations are used for the backward PDEs stemming from the LV and SLV models.

An outline of the rest of our paper is as follows.

In Section 2 a relationship between the forward PDE and backward PDE is introduced, both for the case of the SLV model as for the case of the LV model.

In Section 3 this relationship is preserved at the semidiscrete level: given a spatial discretization of the backward PDE, an adjoint spatial discretization for the forward PDE is defined such that both discretizations yield identical approximations for the fair value of non-path-dependent European options.

In Section 4 an actual spatial discretization, using second-order central finite difference schemes, is constructed for the backward PDE stemming from the SLV model and subsequently the corresponding adjoint spatial discretization is stated.

The main result of the paper is derived in Section 5. It is shown that, under some assumptions, the adjoint spatial discretization can be employed to obtain an expression for the leverage function such that the approximation of the fair value of vanilla options is the same for the LV and SLV models. In order to effectively use this expression, one has to solve a large system of non-linear ordinary differential equations (ODEs).

In Section 6 an Alternating Direction Implicit (ADI) temporal discretization scheme is applied to increase the computational efficiency in the numerical solution of this ODE system and in Section 7 an iteration procedure is described for handling the non-linearity.

In Section 8 ample numerical experiments are presented to illustrate the performance of the obtained SLV calibration procedure.

The final Section 9 gives concluding remarks.

2 Relationship between the forward and the backward Kolmogorov equation

Consider a European-style option with maturity T and payoff u_0 . Denote by $u(x, v, t)$ the *non-discounted fair value* of the option under the SLV model (1.1) at time to maturity t , that is at time level $\tau = T - t$, if $S_\tau = S_0 \exp(x)$ and $V_\tau = v$. It is well-known, see e.g. [4], that the function u satisfies the *backward Kolmogorov equation*

$$\begin{aligned} \frac{\partial}{\partial t} u &= \frac{1}{2} \sigma_{SLV}^2(x, T-t) \psi^2(v) \frac{\partial^2}{\partial x^2} u + \rho \xi \sigma_{SLV}(x, T-t) \psi(v) v^\alpha \frac{\partial^2}{\partial x \partial v} u + \frac{1}{2} \xi^2 v^{2\alpha} \frac{\partial^2}{\partial v^2} u \\ &+ (r_d - r_f - \frac{1}{2} \sigma_{SLV}^2(x, T-t) \psi^2(v)) \frac{\partial}{\partial x} u + \kappa(\eta - v) \frac{\partial}{\partial v} u, \end{aligned} \quad (2.1)$$

for $x, v \in \mathbb{R}$, $0 < t \leq T$. At maturity, i.e. at time level $\tau = T$, the initial condition $u(x, v, 0)$ is defined by the payoff u_0 of the option. By solving PDE (2.1), the fair value $e^{-r_d T} u(X_0, V_0, T)$ of the option under the SLV model can be determined at the spot, i.e. at $\tau = 0$. For strictly positive values of the parameter α , the process V_τ is non-negative and the spatial domain in the v -direction reduces to $v \geq 0$.

If the option under consideration is non-path-dependent, then the payoff u_0 is only a function of (X_T, V_T) , the initial condition is given by $u(x, v, 0) = u_0(x, v)$ and the non-discounted fair value $u(x, v, t)$ of the option can be written as

$$u(x, v, t) = \mathbb{E}[u_0(X_T, V_T) | X_{T-t} = x, V_{T-t} = v],$$

for $0 \leq t \leq T$. By making use of the tower property for conditional expectations it readily follows that

$$u(X_0, V_0, T) = \mathbb{E}[u(X_{T-t}, V_{T-t}, t) | X_0, V_0] = \int_{-\infty}^{\infty} \int_{-\infty}^{\infty} u(x, v, t) p(x, v, T-t; X_0, V_0) dx dv, \quad (2.2)$$

for $0 \leq t \leq T$. Recall that $p(x, v, \tau; X_0, V_0)$ denotes the joint density of (X_τ, V_τ) under the SLV model (1.1). If the parameter α is chosen strictly positive, then the integral with respect to v can be taken from $v = 0$. In particular, the fair value of non-path-dependent European options at the spot can also be computed by evaluating the integral

$$e^{-r_d T} \int_{-\infty}^{\infty} \int_{-\infty}^{\infty} u(x, v, 0) p(x, v, T; X_0, V_0) dx dv, \quad (2.3)$$

where $u(x, v, 0)$ is defined by the payoff of the option.

It can be shown, see e.g. [26], that the joint density $p(x, v, \tau; X_0, V_0)$ satisfies the *forward Kolmogorov equation*

$$\begin{aligned} \frac{\partial}{\partial \tau} p &= \frac{1}{2} \frac{\partial^2}{\partial x^2} (\sigma_{SLV}^2 \psi^2(v) p) + \frac{\partial^2}{\partial x \partial v} (\rho \xi \sigma_{SLV} \psi(v) v^\alpha p) + \frac{1}{2} \frac{\partial^2}{\partial v^2} (\xi^2 v^{2\alpha} p) \\ &\quad - \frac{\partial}{\partial x} ((r_d - r_f - \frac{1}{2} \sigma_{SLV}^2 \psi^2(v)) p) - \frac{\partial}{\partial v} (\kappa(\eta - v) p), \end{aligned} \quad (2.4)$$

for $x, v \in \mathbb{R}$, $\tau > 0$ and with initial condition $p(x, v, 0; X_0, V_0) = \delta(x - X_0) \delta(v - V_0)$ where δ denotes the Dirac delta function. For ease of presentation, the dependency of σ_{SLV} on (x, τ) and the dependency of p on $(x, v, \tau; X_0, V_0)$ is omitted in (2.4). Recall that the process V_τ is non-negative whenever α is strictly positive. In this case the spatial domain of the PDE in the v -direction is naturally restricted to $v \geq 0$. The integrals in (1.5), (2.2), (2.3) with respect to the v -variable can then be taken from 0 to infinity.

Equation (2.2) establishes a *fundamental relationship between the forward and backward Kolmogorov equation*. It states that the fair value of non-path-dependent European options under the SLV model can be seen as the combination of the solution of two different PDEs. By considering the extreme time value $\tau = 0$ ($t = T$), or $\tau = T$ ($t = 0$), only one PDE has to be solved. In the forthcoming sections relationship (2.2) will be employed to define an adjoint spatial discretization for the forward equation.

Even if the functions u and p are known exactly, the integrals in (2.2) can often not be calculated analytically and one relies on numerical integration methods in order to approximate them. In this article we assume that the integrand is known on a Cartesian grid. Denote by m_1 , respectively m_2 , the number of spatial grid points in the x -direction, respectively v -direction. The Cartesian grid is given by

$$(x_i, v_j) \quad \text{for } 1 \leq i \leq m_1, \quad 1 \leq j \leq m_2, \quad (2.5)$$

with $X_{\min} = x_1 < x_2 < \dots < x_{m_1} = X_{\max}$, $V_{\min} = v_1 < v_2 < \dots < v_{m_2} = V_{\max}$ and $X_{\min} < X_0 < X_{\max}$, $V_{\min} < V_0 < V_{\max}$. Define spatial mesh widths $\Delta x_i = x_i - x_{i-1}$ for $2 \leq i \leq m_1$, $\Delta v_j = v_j - v_{j-1}$ for $2 \leq j \leq m_2$ and put $\Delta x_1 = \Delta x_{m_1+1} = \Delta v_1 = \Delta v_{m_2+1} = 0$. When

working with Cartesian grids, most numerical integration methods approximate the expression (2.2) by

$$u(X_0, V_0, T) \approx \sum_{i=1}^{m_1} \sum_{j=1}^{m_2} p(x_i, v_j, T-t; X_0, V_0) u(x_i, v_j, t) w_{x,i} w_{v,j}, \quad (2.6)$$

for certain weights $w_{x,i}, w_{v,j}$. If the numerical integration is performed with the trapezoidal rule, then the weights are given by

$$w_{x,i} = \frac{\Delta x_i + \Delta x_{i+1}}{2} \quad \text{for } 1 \leq i \leq m_1, \quad w_{v,j} = \frac{\Delta v_j + \Delta v_{j+1}}{2} \quad \text{for } 1 \leq j \leq m_2.$$

The values $X_{\min}, V_{\min}, X_{\max}, V_{\max}$ have to lie sufficiently far away from (X_0, V_0) such that the truncation error is negligible. If α is strictly positive, the value V_{\min} can be set equal to zero. In order for (2.6) to be exact if $t = T$ ($\tau = 0$), it is assumed that there exist indices i_0, j_0 such that $(x_{i_0}, v_{j_0}) = (X_0, V_0)$ and the approximation $p(x, v, 0; X_0, V_0) \approx p_0(x, v)$ is used with

$$p_0(x, v) = \begin{cases} \frac{1}{w_{x,i_0} w_{v,j_0}} & \text{if } (x, v) \in [x_{i_0} - \frac{\Delta x_{i_0}}{2}, x_{i_0} + \frac{\Delta x_{i_0+1}}{2}] \times [v_{j_0} - \frac{\Delta v_{j_0}}{2}, v_{j_0} + \frac{\Delta v_{j_0+1}}{2}], \\ 0 & \text{else.} \end{cases}$$

Analogously as above, consider within the LV model a European-style option with payoff $u_{LV,0}$ at maturity T and denote by $u_{LV}(x, t)$ the non-discounted fair value of the option under the LV model (1.2) at time $\tau = T - t$ if $X_{LV,\tau} = x$. The function u_{LV} satisfies the backward Kolmogorov equation

$$\frac{\partial}{\partial t} u_{LV} = \frac{1}{2} \sigma_{LV}^2 \frac{\partial^2}{\partial x^2} u_{LV} + (r_d - r_f - \frac{1}{2} \sigma_{LV}^2) \frac{\partial}{\partial x} u_{LV}, \quad (2.7)$$

for $x \in \mathbb{R}, 0 < t \leq T$ and with initial condition $u_{LV}(x, 0)$ defined by the payoff $u_{LV,0}$ of the option. The non-discounted fair value of the option at the spot ($\tau = 0$) is then given by $u_{LV}(X_0, T)$. For non-path-dependent options this fair value can also be formulated as

$$u(X_0, T) = \int_{-\infty}^{\infty} u_{LV}(x, t) p_{LV}(x, T-t; X_0) dx, \quad (2.8)$$

for $0 \leq t \leq T$, where $p_{LV}(x, \tau; X_0)$ denotes the density of the process $X_{LV,\tau}$ in the LV model (1.2). It can be shown, see e.g. [4], that this density function satisfies the forward Kolmogorov equation

$$\frac{\partial}{\partial \tau} p_{LV} = \frac{1}{2} \frac{\partial^2}{\partial x^2} (\sigma_{LV}^2 p_{LV}) - \frac{\partial}{\partial x} ((r_d - r_f - \frac{1}{2} \sigma_{LV}^2) p_{LV}), \quad (2.9)$$

for $x \in \mathbb{R}, \tau > 0$, and with initial condition $p_{LV}(x, 0; X_0) = \delta(x - X_0)$. Hence, the expression (2.8) establishes a fundamental relationship between the forward and backward Kolmogorov equation which is similar to (2.2). By applying the same numerical integration technique as above, the fair value from (2.8) can be approximated by

$$u(X_0, T) \approx \sum_{i=1}^{m_1} p_{LV}(x_i, T-t; X_0) u(x_i, t) w_{x,i}.$$

Recall that the SLV model is calibrated perfectly to the LV model if the leverage function is defined by (1.4). It was shown by Gyöngy [9] that under this assumption both processes X_τ and $X_{LV,\tau}$ have the same marginal densities, i.e. that

$$\int_{-\infty}^{\infty} p(x, v, \tau; X_0, V_0) dv = p_{LV}(x, \tau; X_0) \quad (2.10)$$

for $x \in \mathbb{R}, \tau \geq 0$. From now on, for the ease of presentation, the dependency of p and p_{LV} on the spot values X_0, V_0 is omitted.

3 Adjoint spatial discretization

In general the values $p(x_i, v_j, \tau)$ and $u(x_i, v_j, t)$ are not known exactly if $\tau > 0$ and $t > 0$, respectively, and one relies on numerical methods to approximate them. Extensive literature is available on numerical techniques to solve backward Kolmogorov equations, see e.g. [30]. A common approach in financial mathematics in order to approximate the fair value of options is by numerically solving the pertinent PDE using the general *method of lines* (MOL), cf. [17]. In this approach, the PDE is first discretized in the spatial variables x and v , yielding a large system of stiff ordinary differential equations (ODEs). This, so-called, *semidiscrete system* is subsequently solved by applying a suitable implicit time stepping method.

Spatial discretization by finite difference or finite volume methods of the backward Kolmogorov equation (2.1) on a Cartesian grid (2.5) yields approximations $\mathbf{U}_{i,j}(t)$ of the exact non-discounted option value $u(x_i, v_j, t)$. Denote by $\mathbf{U}(t)$ the $m_1 \times m_2$ matrix with entries $\mathbf{U}_{i,j}(t)$ and denote by $\mathbf{P}(\tau)$ a matrix with entries $\mathbf{P}_{i,j}(\tau)$ that represent approximations to the exact density values $p(x_i, v_j, \tau)$. In this section, for a general spatial discretization of the backward Kolmogorov equation, an adjoint spatial discretization of the corresponding forward equation is defined such that

$$\sum_{i=1}^{m_1} \sum_{j=1}^{m_2} \mathbf{P}_{i,j}(T-t) \mathbf{U}_{i,j}(t) w_{x,i} w_{v,j} \quad (3.1)$$

is constant for $0 \leq t \leq T$. This can be viewed as a discrete version of relationship (2.2). Consistent *fully discrete* discretizations of the forward and backward Kolmogorov equation have already been considered in the literature, see e.g. [3, 18, 19, 20]. Here, we introduce an adjoint *spatial* discretization that is used in the subsequent sections for the fast, stable and accurate calibration of SLV models.

Let the vector

$$\mathbf{U}(t) = \text{vec}[\mathbf{U}(t)],$$

where $\text{vec}[\cdot]$ denotes the operator that turns any given matrix into a vector by putting its successive columns below each other. Spatial discretization of (2.1) leads to a large system of ODEs of the form

$$\mathbf{U}'(t) = \mathbf{A}^{(B)}(t) \mathbf{U}(t), \quad (3.2)$$

for $0 < t \leq T$, with given matrix $\mathbf{A}^{(B)}(t)$ and with given vector $\mathbf{U}(0)$ that is defined by the payoff of the option. Let the vector

$$\mathbf{P}(\tau) = \text{vec}[\mathbf{P}(\tau)],$$

where the matrix $\mathbf{P}(0)$ is defined by the function p_0 from Section 2. Note that it has only one non-zero entry. Denote by \mathbf{M} the diagonal matrix with diagonal entries

$$M_{k,k} = w_{x,i} w_{v,j},$$

where i, j are the indices such that element $U_k(t)$, respectively $P_k(\tau)$, corresponds to $\mathbf{U}_{i,j}(t)$, respectively $\mathbf{P}_{i,j}(\tau)$. The semidiscrete analogue (3.1) of (2.6) can then be compactly written as

$$u(X_0, V_0, T) \approx \mathbf{P}(T-t)^T \mathbf{M} \mathbf{U}(t), \quad (3.3)$$

where T denotes taking the transpose. If k_0 is the index that corresponds to (i_0, j_0) , then for $t = T$ the right-hand side of (3.3) is equal to $U_{k_0}(T) = \mathbf{U}_{i_0, j_0}(T)$. Now, consider the fair value of any given non-path-dependent European option with maturity T . It is readily seen that semidiscretization of the forward equation (2.4) and semidiscretization of the backward equation (2.1) define *the same approximation* (3.3) of the fair value for all $0 \leq t \leq T$, i.e. property (2.2) holds in the semidiscrete sense, if

$$U_{k_0}(T) = \mathbf{P}(0)^T \mathbf{M} \mathbf{U}(T) = \mathbf{P}(T-t)^T \mathbf{M} \mathbf{U}(t) = \mathbf{P}(\tau)^T \mathbf{M} \mathbf{U}(T-\tau) \quad (3.4)$$

for all $0 \leq t, \tau \leq T$. This requirement is satisfied whenever

$$0 = \mathbf{P}'(\tau)^T \mathbf{M} \mathbf{U}(T-\tau) - \mathbf{P}(\tau)^T \mathbf{M} \mathbf{A}^{(B)}(T-\tau) \mathbf{U}(T-\tau),$$

holds for all $0 \leq \tau \leq T$. Accordingly, we define the *adjoint spatial discretization* of the forward Kolmogorov equation (2.4) as

$$P'(\tau) = M^{-1}(A^{(B)}(T - \tau))^T MP(\tau) \quad \text{for } 0 \leq \tau \leq T, \quad (3.5)$$

In this paper we always employ the adjoint spatial discretization (3.5) of the forward equation. Thus, given any semidiscretization of the backward equation, the obtained approximated option value for non-path-dependent European options satisfy (3.4).

It is convenient to introduce

$$\bar{P}(\tau) = MP(\tau). \quad (3.6)$$

Denote by $\bar{P}(\tau)$ the matrix corresponding to the vector $\bar{P}(\tau)$. The elements $\bar{P}_{i,j}(\tau)$ can be viewed as approximations of

$$\int_{x_i - \frac{\Delta x_i}{2}}^{x_i + \frac{\Delta x_{i+1}}{2}} \int_{v_j - \frac{\Delta v_j}{2}}^{v_j + \frac{\Delta v_{j+1}}{2}} p(x, v, \tau) dx dv,$$

and hence, as an approximation of the probability that

$$(X_\tau, V_\tau) \in [x_i - \frac{\Delta x_i}{2}, x_i + \frac{\Delta x_{i+1}}{2}] \times [v_j - \frac{\Delta v_j}{2}, v_j + \frac{\Delta v_{j+1}}{2}].$$

Clearly,

$$\bar{P}'(\tau) = MM^{-1}(A^{(B)}(T - \tau))^T MP(\tau) = (A^{(B)}(T - \tau))^T \bar{P}(\tau),$$

for $0 \leq \tau \leq T$, with given vector $\bar{P}(0) = MP(0)$, i.e. with

$$\bar{P}_k(0) = \begin{cases} 1 & \text{if } k = k_0, \\ 0 & \text{else.} \end{cases}$$

The approximation (3.3) of the non-discounted fair value of a non-path-dependent European option at the spot can then also be represented as

$$u(X_0, V_0, T) \approx U_{k_0}(T) = \bar{P}(T - t)^T U(t).$$

4 Spatial discretization by finite differences

In this section, a spatial discretization of the backward equation (2.1) by finite differences will be performed on a non-uniform Cartesian grid (2.5). This semidiscretization then defines the adjoint spatial discretization of the forward equation (2.4).

4.1 Spatial discretization of the backward equation

To construct a spatial grid and a semidiscretization for (2.1), the spatial domain needs to be truncated to a bounded set $[X_{\min}, X_{\max}] \times [V_{\min}, V_{\max}]$. The boundaries have to lie sufficiently far away from (X_0, V_0) such that the truncation error incurred is negligible. If the parameter α is strictly positive, the process V_τ is non-negative and V_{\min} is naturally set equal to zero. For non-path-dependent European options the following boundary conditions are imposed:

$$\begin{aligned} \frac{\partial^2}{\partial x^2} u(X_{\min}, v, t) &= \frac{\partial}{\partial x} u(X_{\min}, v, t) & \text{for } 0 \leq v \leq V_{\max}, 0 < t \leq T, \\ \frac{\partial^2}{\partial x^2} u(X_{\max}, v, t) &= \frac{\partial}{\partial x} u(X_{\max}, v, t) & \text{for } 0 \leq v \leq V_{\max}, 0 < t \leq T. \end{aligned} \quad (4.1)$$

The above conditions at $x = X_{\min}$ and $x = X_{\max}$ correspond to linear boundary conditions in the s -variable, where $s = S_0 \exp(x)$, cf. Section 1. If $\alpha = 0$, the process V_τ can take negative values and it is additionally assumed that

$$\begin{aligned} \frac{\partial^2}{\partial v^2} u(x, V_{\min}, t) &= 0 & \text{for } X_{\min} \leq x \leq X_{\max}, 0 < t \leq T, \\ \frac{\partial^2}{\partial v^2} u(x, V_{\max}, t) &= \frac{\partial}{\partial v} u(x, V_{\max}, t) & \text{for } X_{\min} \leq x \leq X_{\max}, 0 < t \leq T. \end{aligned}$$

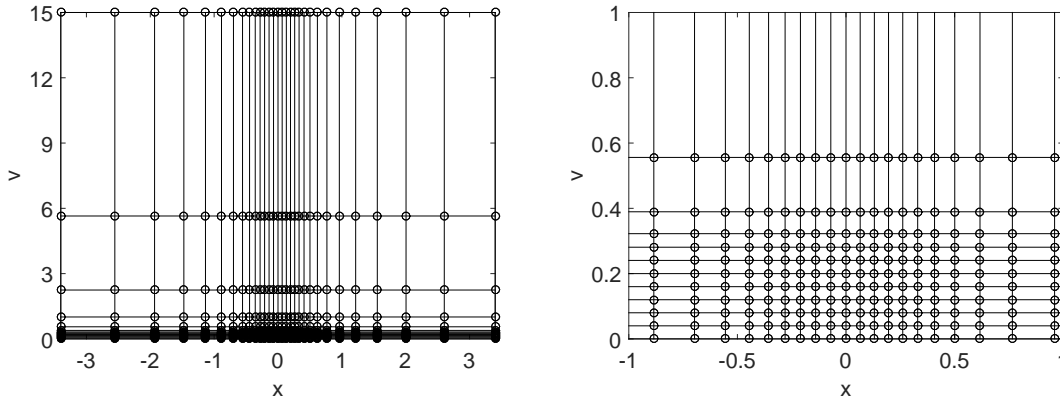


Figure 1: Sample grid for $m_1 = 30, m_2 = 15$, the case $\alpha > 0$, $X_{\min} = -\log(30)$, $X_{\max} = \log(30)$, $V_{\min} = 0$, $V_{\max} = 15$ and $(X_0, V_0) = (0, 0.2)$. The left plot displays the complete grid, the right plot shows the uniformity around (X_0, V_0) .

Thus at $v = V_{\min}$ a linear boundary condition is taken. The condition at $v = V_{\max}$ corresponds with a linear boundary condition in the variable $\exp(v)$. For values of α that are strictly positive, the process V_τ is non-negative. Moreover, $V_\tau = 0$ can be attained if $0 < \alpha \leq 1/2$. In these cases the boundary $v = 0$ of the PDE requires special attention. It has recently been proved in [7] that setting $v = 0$ in the PDE (2.1) at this boundary then yields the correct condition here. At the boundary $v = V_{\max}$ it is then additionally assumed that

$$\frac{\partial^2}{\partial v^2} u(x, V_{\max}, t) = 0 \quad \text{for } X_{\min} \leq x \leq X_{\max}, \quad 0 < t \leq T.$$

For this truncated domain, non-uniform meshes are applied in both the x - and v -direction such that relatively many mesh points lie in the neighbourhood of $x = X_0$ and $v = V_0$. The application of such non-uniform meshes improves the accuracy of the finite difference discretization compared to using uniform meshes. The type of non-uniform meshes that is employed is similar to the ones considered in e.g. [10, 12, 30], which make use of a transformation with the sinh function of an underlying uniform mesh. Akin to [10] we opt to have here a fine, locally uniform mesh around the point $(x, v) = (X_0, V_0)$. Further, the choice $m_1 = 2m_2$ is considered. Denote by $\Delta\xi$ the mesh width of the underlying uniform mesh in the x -direction. Then the mesh under consideration in the x -direction is *smooth* in the sense that there exist real constants $C_0, C_1, C_2 > 0$ such that the mesh widths $\Delta x_i = x_i - x_{i-1}$ satisfy

$$C_0 \Delta\xi \leq \Delta x_i \leq C_1 \Delta\xi \quad \text{and} \quad |\Delta x_{i+1} - \Delta x_i| \leq C_2 (\Delta\xi)^2$$

uniformly in i and m_1 . Analogously, the mesh in the v -direction is smooth. As an illustration, the left plot in Figure 1 displays the spatial grid for the (small) sample values $m_1 = 30, m_2 = 15$, in the case $\alpha > 0$, $X_{\min} = -\log(30)$, $X_{\max} = \log(30)$, $V_{\min} = 0$, $V_{\max} = 15$ and $(X_0, V_0) = (0, 0.2)$. The right plot in Figure 1 displays a part of the spatial grid to show the local uniformity of the grid around (X_0, V_0) .

Semidiscretization on the spatial grid is performed by finite differences. Let $f : \mathbb{R} \rightarrow \mathbb{R}$ be any given function. To approximate the first derivative $f'(x_i)$ we consider two finite difference schemes:

$$f'(x_i) \approx \beta_{i,-1} f(x_{i-1}) + \beta_{i,0} f(x_i) + \beta_{i,1} f(x_{i+1}), \quad (4.2a)$$

$$f'(x_i) \approx \gamma_{i,0} f(x_i) + \gamma_{i,1} f(x_{i+1}) + \gamma_{i,2} f(x_{i+2}), \quad (4.2b)$$

with coefficients given by

$$\begin{aligned}\beta_{i,-1} &= \frac{-\Delta x_{i+1}}{\Delta x_i(\Delta x_i + \Delta x_{i+1})}, & \beta_{i,0} &= \frac{\Delta x_{i+1} - \Delta x_i}{\Delta x_i \Delta x_{i+1}}, & \beta_{i,1} &= \frac{\Delta x_i}{\Delta x_{i+1}(\Delta x_i + \Delta x_{i+1})}, \\ \gamma_{i,0} &= \frac{-2\Delta x_{i+1} - \Delta x_{i+2}}{\Delta x_{i+1}(\Delta x_{i+1} + \Delta x_{i+2})}, & \gamma_{i,1} &= \frac{\Delta x_{i+1} + \Delta x_{i+2}}{\Delta x_{i+1} \Delta x_{i+2}}, & \gamma_{i,2} &= \frac{-\Delta x_{i+1}}{\Delta x_{i+2}(\Delta x_{i+1} + \Delta x_{i+2})}.\end{aligned}$$

To approximate the second derivative $f''(x_i)$, we apply the finite difference scheme

$$f''(x_i) \approx \delta_{i,-1}f(x_{i-1}) + \delta_{i,0}f(x_i) + \delta_{i,1}f(x_{i+1}), \quad (4.3)$$

where

$$\delta_{i,-1} = \frac{2}{\Delta x_i(\Delta x_i + \Delta x_{i+1})}, \quad \delta_{i,0} = \frac{-2}{\Delta x_i \Delta x_{i+1}}, \quad \delta_{i,1} = \frac{2}{\Delta x_{i+1}(\Delta x_i + \Delta x_{i+1})}.$$

The finite difference schemes in the v -direction are defined completely analogously. For a function of two variables $f : \mathbb{R}^2 \rightarrow \mathbb{R}$, the mixed derivative is approximated by application of (4.2a) successively in the two directions. The finite difference schemes above are all well-known. Formula (4.2a), respectively (4.2b), is called the second-order central, respectively second-order forward, formula for the first derivative. Finite difference scheme (4.3) is called the second-order central formula for the second derivative. Through Taylor expansion it can be verified that each of the finite difference approximations above has a second-order truncation error, provided that the function f is sufficiently often continuously differentiable and the mesh is smooth, cf. above.

The actual semidiscretization of the backward PDE (2.1) is defined as follows. At all spatial grid points that do not lie on the boundary of the truncated domain, each spatial derivative appearing in (2.1) is replaced by its corresponding second-order central finite difference scheme described above.

Concerning the boundaries in the x -direction, it is assumed that the pertinent conditions from (4.1) are valid for every x smaller than x_2 or larger than x_{m_1-1} . Thus for these extreme values x we assume that $u(\cdot, v, t)$ is an exponential function. For instance, considering the upper boundary

$$u_x = u_{xx} = C_{b,1} \exp(x) \quad \text{whenever } x > x_{m_1-1},$$

and hence

$$u = C_{b,1} \exp(x) + C_{b,2} \quad \text{whenever } x > x_{m_1-1},$$

for some constants $C_{b,1}$, $C_{b,2}$. Based on the function values u at x_{m_1-1} and x_{m_1} the constants $C_{b,1}$, $C_{b,2}$ can be determined and this leads to the approximation for both the first and second derivatives in the x -direction at x_{m_1} given by

$$C_{b,1} \exp(x_{m_1}) = \frac{-\exp(x_{m_1})}{\exp(x_{m_1}) - \exp(x_{m_1-1})} u(x_{m_1-1}, v, t) + \frac{\exp(x_{m_1})}{\exp(x_{m_1}) - \exp(x_{m_1-1})} u(x_{m_1}, v, t).$$

The first and second derivatives in the x -direction at the lower boundary are approximated analogously.

If the parameter α is strictly positive, a linear boundary condition is applied at $v = V_{\max}$, i.e. the second derivative in the v -direction is equal to zero. The first derivative in the v -direction at this boundary is approximated by using the central scheme (4.2a) with the virtual point $V_{\max} + \Delta v_{m_2}$, where the value at this point is defined by extrapolation using the linear boundary condition. This discretization reduces to the first-order backward finite difference formula for the first derivative. Moreover, at the boundary $V_{\min} = 0$ all the second derivatives vanish and the first derivative $\partial u / \partial v$ is then approximated by using the forward scheme (4.2b). If α equals zero, a linear boundary condition is imposed at V_{\min} and discretization of the spatial derivatives in the v -direction is performed as above. The discretization of the boundary condition at V_{\max} is then performed analogously as the discretization of the boundary conditions in the x -direction.

Denote by D_x , respectively D_{xx} , the matrices corresponding with the first, respectively second, derivatives in the x -direction. Analogously, denote by D_v, D_{vv} the matrices corresponding with

spatial derivatives in the v -direction. For example, given that $\alpha > 0$, D_v is the matrix with entries

$$\begin{aligned}(D_v)_{1,1} &= \frac{-2\Delta v_2 - \Delta v_3}{\Delta v_2(\Delta v_2 + \Delta v_3)}, & (D_v)_{1,2} &= \frac{\Delta v_2 + \Delta v_3}{\Delta v_2 \Delta v_3}, & (D_v)_{1,3} &= \frac{-\Delta v_2}{\Delta v_3(\Delta v_2 + \Delta v_3)}, \\ (D_v)_{i,i-1} &= \frac{-\Delta v_{i+1}}{\Delta v_i(\Delta v_i + \Delta v_{i+1})}, & (D_v)_{i,i} &= \frac{\Delta v_{i+1} - \Delta v_i}{\Delta v_i \Delta v_{i+1}}, & (D_v)_{i,i+1} &= \frac{\Delta v_i}{\Delta v_{i+1}(\Delta v_i + \Delta v_{i+1})}, \\ (D_v)_{m_2, m_2-1} &= \frac{-1}{\Delta v_{m_2}}, & (D_v)_{m_2, m_2} &= \frac{1}{\Delta v_{m_2}},\end{aligned}$$

where $i \in \{2, \dots, m_2 - 1\}$. Denote by $L(\tau)$ the $m_1 \times m_1$ diagonal matrix with entries $\sigma_{SLV}(x_i, \tau)$, let Λ be the $m_2 \times m_2$ diagonal matrix with entries v_j , and define for an arbitrary function $f : \mathbb{R} \rightarrow \mathbb{R}$ the matrix $f(\Lambda)$ as the diagonal matrix with entries $f(v_j)$. Further, denote by I_x , respectively I_v , the identity matrix of size $m_1 \times m_1$, respectively $m_2 \times m_2$. Then semidiscretization of (2.1) yields a system of differential equations given by

$$\begin{aligned}U'(t) &= \frac{1}{2}L^2(T-t)D_{xx}U(t)\psi^2(\Lambda) + \rho\xi L(T-t)D_xU(t)D_v^T\Lambda^\alpha\psi(\Lambda) + \frac{1}{2}\xi^2U(t)D_{vv}^T\Lambda^{2\alpha} \\ &\quad + (r_d - r_f)D_xU(t) - \frac{1}{2}L^2(T-t)D_xU(t)\psi^2(\Lambda) + U(t)D_v^T\kappa(\eta I_v - \Lambda),\end{aligned}$$

for $0 < t \leq T$. This can be written in the form (3.2),

$$U'(t) = A^{(B)}(t)U(t) = (A_0^{(B)}(t) + A_1^{(B)}(t) + A_2^{(B)}(t))U(t) \quad (4.4)$$

for $0 < t \leq T$ where, using a well-known property of the *Kronecker product* \otimes ,

$$\begin{aligned}A_0^{(B)}(t) &= (\rho\xi\psi(\Lambda)\Lambda^\alpha D_v) \otimes (L(T-t)D_x), \\ A_1^{(B)}(t) &= \frac{1}{2}\psi^2(\Lambda) \otimes (L^2(T-t)D_{xx}) + (r_d - r_f)I_v \otimes D_x - \frac{1}{2}\psi^2(\Lambda) \otimes (L^2(T-t)D_x), \\ A_2^{(B)}(t) &= (\frac{1}{2}\xi^2\Lambda^{2\alpha}D_{vv} + \kappa(\eta I_v - \Lambda)D_v) \otimes I_x.\end{aligned}$$

The initial vector $U(0)$ is defined by the payoff of the option.

4.2 Spatial discretization of the forward equation

As indicated in Section 3, semidiscretization of the forward equation (2.4) is performed by the adjoint spatial discretization (3.5). Since the transpose of the Kronecker product of two matrices is equal to the Kronecker product of the transposed matrices, and recalling that $t = T - \tau$, it follows that $\bar{P}(\tau)$ defined by (3.6) is given by the system of ODEs

$$\bar{P}'(\tau) = \bar{A}^{(F)}(\tau)\bar{P}(\tau) = (\bar{A}_0^{(F)}(\tau) + \bar{A}_1^{(F)}(\tau) + \bar{A}_2^{(F)}(\tau))\bar{P}(\tau), \quad (4.5)$$

for $\tau > 0$, with

$$\begin{aligned}\bar{A}_0^{(F)}(\tau) &= (\rho\xi D_v^T\Lambda^\alpha\psi(\Lambda)) \otimes (D_x^T L(\tau)), \\ \bar{A}_1^{(F)}(\tau) &= \frac{1}{2}\psi^2(\Lambda) \otimes (D_{xx}^T L^2(\tau)) + (r_d - r_f)I_v \otimes D_x^T - \frac{1}{2}\psi^2(\Lambda) \otimes (D_x^T L^2(\tau)), \\ \bar{A}_2^{(F)}(\tau) &= (\frac{1}{2}\xi^2 D_{vv}^T\Lambda^{2\alpha} + D_v^T\kappa(\eta I_v - \Lambda)) \otimes I_x,\end{aligned}$$

and given initial vector $\bar{P}(0)$. This in turn corresponds to the system of differential equations

$$\begin{aligned}\bar{P}'(\tau) &= \frac{1}{2}D_{xx}^T L^2(\tau)\bar{P}(\tau)\psi^2(\Lambda) + \rho\xi D_x^T L(\tau)\bar{P}(\tau)\psi(\Lambda)\Lambda^\alpha D_v + \frac{1}{2}\xi^2\bar{P}(\tau)\Lambda^{2\alpha}D_{vv} \\ &\quad + (r_d - r_f)D_x^T\bar{P}(\tau) - \frac{1}{2}D_x^T L^2(\tau)\bar{P}(\tau)\psi^2(\Lambda) + \bar{P}(\tau)\kappa(\eta I_v - \Lambda)D_v,\end{aligned} \quad (4.6)$$

for $\tau > 0$. The expression (4.6) shall be employed to calibrate the SLV model to the LV model.

The total integral of a density function is equal to one. For a natural adjoint spatial discretization (4.5) one would expect that the total numerical integral of \bar{P} , corresponding with \bar{P} , is close

to one. Let e_x and e_v denote the vectors consisting of all ones with lengths m_1 and m_2 , respectively. By construction of the finite difference discretization and the chosen boundary conditions for the SLV model (2.1) there holds

$$D_{xx}e_x = D_x e_x = 0 \quad \text{and} \quad D_{vv}e_v = D_v e_v = 0 \quad (4.7)$$

and it directly follows that

$$e_x^T \bar{P}'(\tau) e_v = 0$$

for all $\tau > 0$. Since further $e_x^T \bar{P}(0) e_v = 1$, this yields

$$\sum_{i=1}^{m_1} \sum_{j=1}^{m_2} P_{i,j}(\tau) w_{x,i} w_{v,j} = \sum_{i=1}^{m_1} \sum_{j=1}^{m_2} \bar{P}_{i,j}(\tau) = 1$$

for all $\tau \geq 0$. It can be concluded that the adjoint spatial discretization of the forward Kolmogorov equation keeps the total numerical integral of the density identically equal to one, which is a favourable property.

5 Matching the semidiscrete LV and SLV models

In this section the main result of the article is presented. It is shown that, under some assumptions, one can calibrate the semidiscrete SLV model exactly to the corresponding semidiscrete LV model.

A priori the leverage function σ_{SLV} , and hence the matrix function L , are unknown and one wishes to determine them in such a way that the LV model and the SLV model define identical values for European call and put options. In practice, however, even the LV function σ_{LV} is not known analytically in general and one relies on numerical methods to approximate the option value defined by the LV model. Accordingly, it is unrealistic to require an algorithm to produce a leverage function σ_{SLV} such that the SLV model yields the same exact European call and put values as the LV model. One rather wants to construct the leverage function in such a way that the two models yield *identical approximate values* for European call and put options whenever similar semidiscretizations of these models are used.

A common approach to approximate the fair value of a European-style option under the LV model is by discretizing the backward PDE (2.7) with finite differences. Since the region of interest in the x -direction in the LV model is the same as that in the SLV model, the same spatial mesh can be used in this spatial direction. Denote by $U_{LV}(t)$ the vector with approximations $U_{LV,i}(t)$ to $u_{LV}(x_i, t)$ for $1 \leq i \leq m_1$ such that the component $U_{LV,i_0}(T)$ is the approximation of the non-discounted fair value at the spot. Semidiscretization by finite differences then leads to a system of ODEs

$$U'_{LV}(t) = A_{LV}^{(B)}(t) U_{LV}(t) \quad (5.1)$$

for $0 < t \leq T$, with initial vector $U_{LV}(0)$ defined by the payoff $u_{LV,0}$. Since the spatial derivatives $\partial/\partial x$ and $\partial^2/\partial x^2$ in (2.7) also occur in the backward equation (2.1), and since also the same boundary conditions from Section 4 can be applied for non-path-dependent European options, the same finite difference matrices D_x and D_{xx} can be used to perform semidiscretization, and hence

$$A_{LV}^{(B)}(t) = \frac{1}{2} L_{LV}^2(T-t) D_{xx} + (r_d - r_f) D_x - \frac{1}{2} L_{LV}^2(T-t) D_x,$$

where $L_{LV}(\tau)$ is the $m_1 \times m_1$ diagonal matrix with entries $\sigma_{LV}(x_i, \tau)$.

Denote by $P_{LV}(\tau)$ a vector with approximations $P_{LV,i}(\tau)$ of $p_{LV}(x_i, \tau)$, where p_{LV} is given by the forward equation (2.9), and define $\bar{P}_{LV}(\tau) = M_{LV} P_{LV}(\tau)$ where M_{LV} is the diagonal matrix with entries

$$(M_{LV})_{i,i} = w_{x,i}, \quad \text{for } 1 \leq i \leq m_1.$$

Analogously to Section 3, we define an adjoint forward discretization by

$$\bar{P}'_{LV}(\tau) = (A_{LV}^{(B)}(T-\tau))^T \bar{P}_{LV}(\tau) = \bar{A}_{LV}^{(F)}(\tau) \bar{P}_{LV}(\tau) \quad (5.2)$$

for $\tau > 0$, with

$$\bar{A}_{LV}^{(F)}(\tau) = \frac{1}{2}D_{xx}^T L_{LV}^2(\tau) + (r_d - r_f)D_x^T - \frac{1}{2}D_x^T L_{LV}^2(\tau),$$

and

$$\bar{P}_{LV,i}(0) = \begin{cases} 1 & \text{if } i = i_0, \\ 0 & \text{else,} \end{cases}$$

so that

$$U_{LV,i_0}(T) = \bar{P}_{LV}(T-t)^T U_{LV}(t)$$

for all $0 \leq t \leq T$. Especially, for non-path-dependent European options one can just solve the forward problem and approximate the non-discounted fair value at the spot by $\bar{P}_{LV}(T)^T U_{LV}(0)$.

Now, consider a non-path-dependent option whose payoff is only dependent on the exchange rate S_T . Then

$$U_{LV,i}(0) = U_{i,j}(0)$$

whenever $1 \leq i \leq m_1, 1 \leq j \leq m_2$. It is readily verified that the semidiscretizations of the LV model and the SLV model define the same value at the spot, i.e. $U_{LV,i_0}(T) = U_{i_0,j_0}(T)$, if

$$\bar{\mathbf{P}}(T)e_v = \bar{P}_{LV}(T).$$

This property is desirable for every possible maturity. Hence, one would like to have

$$\bar{\mathbf{P}}(\tau)e_v = \bar{P}_{LV}(\tau) \tag{5.3}$$

for all $\tau \geq 0$. Notice that (5.3) is equivalent to

$$\sum_{j=1}^{m_2} \mathbf{P}_{i,j}(\tau)w_{v,j} = P_{LV,i}(\tau) \quad \text{for } 1 \leq i \leq m_1, \tau \geq 0,$$

which can be viewed as a semidiscrete analogue of (2.10). Since $\bar{\mathbf{P}}(0)e_v = \bar{P}_{LV}(0)$, the condition (5.3) is satisfied if

$$\bar{\mathbf{P}}'(\tau)e_v = \bar{P}'_{LV}(\tau) \tag{5.4}$$

for all $\tau > 0$. From (4.6), (4.7) we directly obtain

$$\bar{\mathbf{P}}'(\tau)e_v = \frac{1}{2}D_{xx}^T L^2(\tau)\bar{\mathbf{P}}(\tau)\psi^2(\Lambda)e_v + (r_d - r_f)D_x^T \bar{\mathbf{P}}(\tau)e_v - \frac{1}{2}D_x^T L^2(\tau)\bar{\mathbf{P}}(\tau)\psi^2(\Lambda)e_v.$$

If the (initially unspecified) diagonal matrix $L(\tau)$ is now defined through

$$L^2(\tau)\bar{\mathbf{P}}(\tau)\psi^2(\Lambda)e_v = L_{LV}^2(\tau)\bar{\mathbf{P}}(\tau)e_v, \tag{5.5}$$

then

$$\bar{\mathbf{P}}'(\tau)e_v = \frac{1}{2}D_{xx}^T L_{LV}^2(\tau)\bar{\mathbf{P}}(\tau)e_v + (r_d - r_f)D_x^T \bar{\mathbf{P}}(\tau)e_v - \frac{1}{2}D_x^T L_{LV}^2(\tau)\bar{\mathbf{P}}(\tau)e_v.$$

Hence, it follows that (5.4) holds whenever equation (5.2) has a unique solution.

Remark that in the definition (5.5) for the semidiscrete leverage function it is tacitly assumed that both vectors

$$\bar{\mathbf{P}}(\tau)\psi^2(\Lambda)e_v \quad \text{and} \quad \bar{\mathbf{P}}(\tau)e_v$$

only contain strictly positive values. By performing a spatial discretization with finite differences it is possible that some of the values $\bar{\mathbf{P}}_{i,j}$ become negative. In our experiments, both vectors often remained strictly positive for natural values of m_1, m_2 .

Notice that *the derivation above is not restricted to the choice of finite difference formulas*. If the second-order central formulas from Subsection 4.1 are replaced by alternative finite difference formulas for which (4.7) holds, and if these formulas are also applied for a similar semidiscretization in the LV model, then the SLV model is calibrated exactly to the LV model by employing (5.5).

We arrive at the following main result.

Theorem 5.1 *Assume semidiscretization of the backward Kolmogorov equation (2.1) is performed by consistent finite difference formulas on a Cartesian grid and that semidiscretization of the forward Kolmogorov equation (2.4) is performed by the adjoint spatial discretization. Then*

$$U_{k_0}(T) = \bar{P}(\tau)^T U(T - \tau) \quad \text{for all } 0 \leq \tau \leq T,$$

where k_0 corresponds to the index (i_0, j_0) such that $(x_{i_0}, v_{j_0}) = (X_0, V_0)$. Hence, the two semidiscretizations define the same approximation for the fair value of non-path-dependent European options.

Next, assume semidiscretization of the backward and forward equations (2.7) and (2.9) under the LV model is performed in complete correspondence to that of (2.1) and (2.4), respectively, under the SLV model by using the same grid and finite difference formulas in the x -direction. If (4.7) holds and equation (5.2) has a unique solution and if the leverage function σ_{SLV} is defined on the grid in the x -direction by

$$\sigma_{SLV}^2(x_i, \tau) = \sigma_{LV}^2(x_i, \tau) \frac{\sum_{j=1}^{m_2} \bar{P}_{i,j}(\tau)}{\sum_{j=1}^{m_2} \psi^2(v_j) \bar{P}_{i,j}(\tau)}, \quad (5.6)$$

then

$$\bar{P}(\tau) e_v = \bar{P}_{LV}(\tau) \quad \text{for all } \tau \geq 0.$$

In particular, if the payoff depends only on the exchange rate S_T , then the semidiscretizations of the LV model and the SLV model define the same approximation for the fair value of non-path-dependent European options:

$$U_{LV, i_0}(T) = \bar{P}_{LV}(\tau)^T U_{LV}(T - \tau) = \bar{P}(\tau)^T U(T - \tau) = U_{k_0}(T) \quad \text{for all } 0 \leq \tau \leq T.$$

The second part of Theorem 5.1 can be regarded as the semidiscrete analogue of (1.4). Indeed, if σ_{SLV} is defined on the spatial grid in the x -direction by (5.6), then by the definition of \bar{P} it is directly seen that this is equivalent to applying (1.4), where the conditional expectation is approximated by

$$\mathbb{E}[\psi^2(V_\tau) | X_\tau = x_i] \approx \frac{\sum_{j=1}^{m_2} \psi^2(v_j) P_{i,j}(\tau) w_{v,j}}{\sum_{j=1}^{m_2} P_{i,j}(\tau) w_{v,j}} = \frac{\sum_{j=1}^{m_2} \psi^2(v_j) \bar{P}_{i,j}(\tau)}{\sum_{j=1}^{m_2} \bar{P}_{i,j}(\tau)} \quad \text{for } 1 \leq i \leq m_1. \quad (5.7)$$

6 Time discretization

In this section we consider a suitable time stepping method for the numerical solution of semidiscrete systems of the type (4.4) and (4.5) assuming that the matrix-valued function L is known. In general, semidiscretization by means of finite difference or finite volume methods of initial-boundary value problems for two-dimensional time-dependent convection-diffusion equations leads to large systems of stiff ODEs,

$$W'(t) = F(t, W(t)) \quad (0 < t \leq T), \quad W(0) = W_0,$$

with given vector-valued function $F : [0, T] \times \mathbb{R}^m \rightarrow \mathbb{R}^m$ and given vector $W_0 \in \mathbb{R}^m$ where $m \geq 1$ is the number of spatial grid points. For the effective time discretization of these semidiscrete systems, *operator splitting schemes* of the *Alternating Direction Implicit* (ADI) type are widely used in practice. Several ADI schemes have been developed and analyzed in the literature for the situation where mixed spatial derivative terms are present in the convection-diffusion equation. Mixed derivative terms are ubiquitous in the field of financial option valuation; they arise due to correlations between the underlying stochastic processes. Notably, this holds for the general SLV model (1.1) under consideration.

In this paper we employ the *Modified Craig-Sneyd (MCS) scheme*, which is a modern scheme of the ADI-type suitable to deal with mixed derivative terms. Let the vector-valued function F be decomposed as

$$F(t, w) = F_0(t, w) + F_1(t, w) + F_2(t, w) \quad (0 \leq t \leq T, w \in \mathbb{R}^m),$$

where F_0 represents the mixed spatial derivative term and F_1 , respectively F_2 , represents all spatial derivative terms in the first, respectively second, spatial direction. Let $\theta > 0$ be a given parameter, $N \geq 1$ the number of time steps and $t_n = n\Delta t$ with $\Delta t = T/N$. Then the MCS scheme defines approximations W_n to $W(t_n)$ successively for $n = 1, 2, 3, \dots, N$ through

$$\left\{ \begin{array}{l} Y_0 = W_{n-1} + \Delta t F(t_{n-1}, W_{n-1}), \\ Y_l = Y_{l-1} + \theta \Delta t (F_l(t_n, Y_l) - F_l(t_{n-1}, W_{n-1})), \quad l = 1, 2, \\ \hat{Y}_0 = Y_0 + \theta \Delta t (F_0(t_n, Y_2) - F_0(t_{n-1}, W_{n-1})), \\ \tilde{Y}_0 = \hat{Y}_0 + (\frac{1}{2} - \theta) \Delta t (F(t_n, Y_2) - F(t_{n-1}, W_{n-1})), \\ \tilde{Y}_l = \tilde{Y}_{l-1} + \theta \Delta t (F_l(t_n, \tilde{Y}_l) - F_l(t_{n-1}, W_{n-1})), \quad l = 1, 2, \\ W_n = \tilde{Y}_2. \end{array} \right. \quad (6.1)$$

The MCS scheme (6.1) has been introduced by in 't Hout & Welfert [15]. It starts with an explicit Euler predictor stage, which is followed by two implicit but unidirectional corrector stages. Then a second explicit stage is performed, followed again by two implicit unidirectional corrector stages. In the special case where $\theta = \frac{1}{2}$ one obtains the *Craig-Sneyd (CS) scheme*, proposed in [5]. Observe the favourable feature that the F_0 part, representing the mixed derivative term, is always treated in an explicit manner.

In the past years various positive *stability* results have been derived for the MCS scheme relevant to multidimensional convection-diffusion equations with mixed derivative terms, see e.g. [13, 14, 15, 22]. Subsequently, in 't Hout & Wyns [16] proved that, under natural stability and smoothness assumptions, the MCS scheme is *second-order convergent* with respect to the time step whenever it is applied to semidiscrete two-dimensional convection-diffusion equations with mixed derivative term. The temporal convergence bound from [16] has the key property that it holds uniformly in the spatial mesh width.

In the present application, both vectors $U(0)$ and $\bar{P}(0)$ are stemming from initial functions that are nonsmooth. It is well-known in the literature that the convergence behaviour of time discretization methods can be seriously impaired for nonsmooth initial data, compare [23, 32]. To alleviate this, Rannacher time stepping will be applied, that is, the first few time steps of the MCS scheme are replaced by twice as many half time steps using the implicit Euler scheme [24]. We opt to replace here the first two MCS time steps by four half time steps of the implicit Euler scheme. Based on the recent results in [32], the MCS scheme is then expected to maintain second-order convergence in time, uniformly in the number of spatial grid points.

As seen in Section 2, the fair values of non-path-dependent European options can be determined by solving either the backward equation (2.1) or the forward equation (2.4). In Section 4 spatial discretization of these two PDEs led to the semidiscrete systems (4.4) and (4.5), respectively. Application of the MCS scheme to (4.4) yields approximations U_n of $U(t_n)$ and the non-discounted fair option value at the spot is then approximated by $U_{k_0, N} = \bar{P}_0^T U_N$. Alternatively, take $\Delta\tau = \Delta t = T/N$ and let temporal grid points $\tau_n = n\Delta\tau = T - t_{N-n}$. Application of the MCS scheme to (4.5) yields approximations \bar{P}_n of $\bar{P}(\tau_n)$ and the non-discounted fair option value at the spot is then approximated by $\bar{P}_N^T U_0$.

It is possible, see Itkin [18, 19], to construct new ADI discretizations for (4.5) such that there is an exact match between the fully discretized backward equation and the fully discretized forward

equation, that is,

$$\bar{P}_0^T U_N = \bar{P}_N^T U_0 = \bar{P}_{N-n}^T U_n$$

for all $0 \leq n \leq N$. In this paper we prefer to employ the MCS scheme for the numerical solution of both ODE systems (4.4) and (4.5). A main reason is that ample positive results are already available in the literature on the stability and convergence of the MCS scheme. In addition, practical experience shows that the temporal discretization error of the MCS scheme is often much smaller than the spatial discretization error.

7 Calibration of the SLV model to the LV model

In Section 5 we derived the expression (5.6) for the discrete leverage function σ_{SLV} that exactly calibrates the semidiscrete SLV model to the semidiscrete LV model. This expression involves the matrix function \bar{P} . Combining (5.6) with the semidiscrete forward equation (4.5) for $\bar{P} = \text{vec}[\bar{P}]$, one arrives at a large, non-linear system of ODEs. In the present section numerical time-stepping is applied together with an inner iteration so as to numerically solve this system of ODEs and acquire the discrete leverage function that satisfies (5.6).

Suppose an approximation \bar{P}_n to $\bar{P}(\tau_n)$ at time level τ_n is known. Let \bar{P}_n denote the $m_1 \times m_2$ matrix such that

$$\bar{P}_n = \text{vec}[\bar{P}_n].$$

Then the discrete leverage function is determined by

$$\sigma_{SLV}^2(x_i, \tau_n) \mathbb{E}_{n,i} = \sigma_{LV}^2(x_i, \tau_n), \quad (7.1)$$

where the quantity

$$\mathbb{E}_{n,i} = \frac{\sum_{j=1}^{m_2} \psi^2(v_j) \bar{P}_{n,i,j}}{\sum_{j=1}^{m_2} \bar{P}_{n,i,j}} \quad (7.2)$$

forms an approximation to the conditional expectation $\mathbb{E}[\psi^2(V_{\tau_n}) | X_{\tau_n} = x_i]$, see (5.7). In order to arrive at the actual calibration procedure, we need to consider three practical issues concerning formula (7.2).

- Due to the spatial and temporal discretizations, it may happen that either the numerator or denominator of (7.2) becomes negative. In this case we assume that the conditional expectation is locally constant in time and set $\mathbb{E}_{n,i} = \mathbb{E}_{n-1,i}$. In most of our experiments, however, both parts of the quotient remained strictly positive for common values of $m_1, m_2, \Delta\tau$.

- Since $\bar{P}_{n,i,j}$ is an approximation of the probability of the event that

$$(X_{\tau_n}, V_{\tau_n}) \in [x_i - \frac{\Delta x_i}{2}, x_i + \frac{\Delta x_{i+1}}{2}] \times [v_j - \frac{\Delta v_j}{2}, v_j + \frac{\Delta v_{j+1}}{2}],$$

it can happen that both the numerator and denominator of (7.2) become very small, which can lead to unrealistic values of the leverage function. To resolve this, a regularized approximation of the conditional expectation is used (cf. [8]),

$$\mathbb{E}_{n,i} = \frac{\sum_{j=1}^{m_2} \psi^2(v_j) \bar{P}_{n,i,j} + \psi^2(\eta) \epsilon}{\sum_{j=1}^{m_2} \bar{P}_{n,i,j} + \epsilon} \quad (7.3)$$

for given small value ϵ . In this paper $\epsilon = 10^{-8}$ is taken. By using the regularized version (7.3), the approximated conditional expectation is shifted towards $\psi^2(\eta)$ where η is the mean-reversion level of the process V_τ .

- At the spot $\tau = 0$, the matrix $\bar{P}(0)$ has (i_0, j_0) -th entry equal to one and all its other entries are equal to zero. Consequently, if $n = 0$, then the expression (7.2) is only defined if $i = i_0$. To render the calibration procedure feasible, we extend this definition to all indices i and thus put

$$\mathbb{E}_{0,i} = \psi^2(V_0).$$

Notice that this agrees with (7.3) for $n = 0$ whenever $\eta = V_0$, which often holds in practice.

Let $Q \geq 1$ be a given integer. For calibrating the SLV model to the LV model, we employ the following numerical procedure. It consists of numerical time stepping combined with an inner iteration, cf. [29].

```

for  $n$  is 1 to  $N$  do
    let  $\bar{P}_n = \bar{P}_{n-1}$  be an initial approximation to  $\bar{P}(\tau_n)$ ;

    for  $q$  is 1 to  $Q$  do
        (a) approximate the conditional expectations  $\mathbb{E}[\psi^2(V_{\tau_n})|X_{\tau_n} = x_i]$  by (7.3);
        (b) approximate  $\sigma_{SLV}(\cdot, \tau_n)$  on the grid in the  $x$ -direction by formula (7.1);
        (c) update  $\bar{P}_n$  by performing a numerical time step for (4.5) from  $\tau_{n-1}$  to  $\tau_n$ ;
    end
end

```

Whenever a time step from τ_{n-1} to τ_n with the MCS scheme is replaced by two half-time steps of the implicit Euler scheme, the inner iteration above is first performed for the substep from τ_{n-1} to $\tau_{n-1/2} = \tau_{n-1} + \Delta\tau/2$, yielding an approximation of $\bar{P}(\tau_{n-1/2})$ and $\sigma_{SLV}(\cdot, \tau_{n-1/2})$. Next, the inner iteration is performed for the substep from $\tau_{n-1/2}$ to τ_n , yielding an approximation of $\bar{P}(\tau_n)$ and $\sigma_{SLV}(\cdot, \tau_n)$.

Upon completion of the time stepping and iteration procedure above, the original approximation for $\sigma_{SLV}(\cdot, 0)$ is replaced on the grid in the x -direction by

$$\sigma_{LV}^2(x_i, 0) = \sigma_{SLV}^2(x_i, 0) \frac{\sum_{j=1}^{m_2} \psi^2(v_j) \bar{P}_{i,j,1} + \psi^2(\eta) \epsilon}{\sum_{j=1}^{m_2} \bar{P}_{i,j,1} + \epsilon}$$

for $1 \leq i \leq m_1$. This appears more realistic as the original approximation was actually only valid for the index $i = i_0$.

8 Numerical experiments

In this section, numerical experiments are presented to illustrate the effectiveness of the calibration procedure. Here, we opt to consider the popular and challenging Heston-based SLV model, i.e. SLV model (1.1) with $\psi(v) = \sqrt{v}$ and $\alpha = 1/2$, to describe the evolution of the EUR/USD exchange rate.

As stated in the introduction, for the calibration of the SLV model it is customary to start from the parameters κ, η, ξ, ρ of the underlying (Heston) SV model such that this model reflects the market dynamics of the exchange rate. In this article we consider the following four sets of parameters:

	κ	η	ξ	ρ	T	$2\kappa\eta/\xi^2$
Case 1	3.02	0.015	0.31	-0.13	$6M$	0.9428
Case 2	0.30	0.04	0.90	-0.5	$6M$	0.0296
Case 3	0.75	0.015	0.15	-0.14	$2Y$	1
Case 4	0.30	0.04	0.90	-0.5	$2Y$	0.0296

The first and third parameter set are taken from [4, Table 6.5]. They correspond to the EUR/USD exchange rate for the pertinent maturities (market data as of 16 September 2008). The second and fourth parameter set are essentially the same and taken from [2, Case II]. The latter two

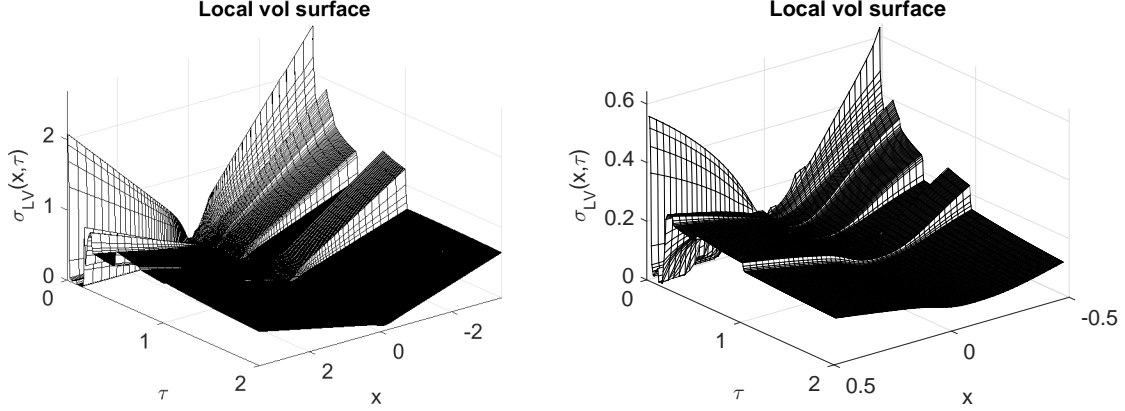


Figure 2: Local volatility function originating from actual EUR/USD vanilla option data (market data as of 13 November 2015) on the full domain in the x -direction (left) and on a subdomain around the spot rate (right). The spot rate $S_0 = 1.0764$.

sets are challenging for the calibration procedure as the *Feller condition* is strongly violated, i.e. $2\kappa\eta/\xi^2 \ll 1$, so that the probability mass is stacked up near $v = 0$, cf. [1]. Note that the spatial discretization of the backward Kolmogorov equation (2.1) from Subsection 4.1, and hence the total calibration procedure, is not dependent on the Feller condition.

The leverage function σ_{SLV} is determined in such a way that the SLV model is calibrated exactly to the underlying LV model. The LV model is completely determined by the LV function σ_{LV} and the risk-free interest rates r_d, r_f . For the experiments we consider

$$r_d = 0.03, \quad r_f = 0.01,$$

and LV function displayed in Figure 2. This LV function originates from actual EUR/USD vanilla option data (market data as of 13 November 2015) and contains data up to two year. The corresponding spot rate is

$$S_0 = 1.0764.$$

For the spot value V_0 of the process V_τ in the SLV model we assume that it is equal to the long-term mean η of this process.

The aim is to construct the leverage function in such a way that the discretized LV model and the discretized SLV model yield identical approximate values for any given vanilla option whenever similar discretizations are employed. In our experiments, the semidiscretization of the backward Kolmogorov equation (2.1) is performed as described in Subsection 4.1 and the semidiscretization of the forward equation (2.4) is defined by the pertinent adjoint spatial discretization. The backward and forward PDEs (2.7) and (2.9) are semidiscretized analogously and by using the same finite difference schemes as described in Section 5. For the first numerical experiment we consider

$$m_1 = 100, \quad m_2 = 50.$$

The main Theorem 5.1 yields that if the leverage function is defined on the grid in the x -direction by (5.6), then the approximations obtained from the four semidiscrete systems (4.4), (4.5), (5.1), (5.2) of the fair value of any given non-path-dependent European option are identical. The exact solution (5.6) is approximated by applying the calibration procedure described in Section 7. We choose to perform the temporal discretization in this procedure with values

$$\Delta\tau = 1/200, \quad \theta = 1/3, \quad Q = 2.$$

In Figure 3 the obtained discrete leverage function is shown for Case 4. If the SV model with

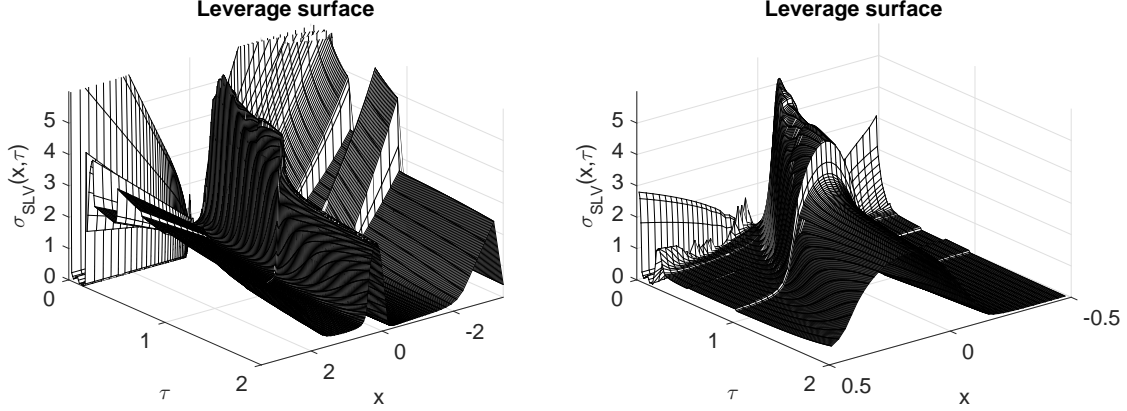


Figure 3: Leverage function on the full domain in the x -direction (left) and on a subdomain around the spot rate (right), stemming from the calibration procedure with local volatility function from Figure 2, SV parameters from Case 4 and with $m_1 = 100$, $m_2 = 50$, $\Delta\tau = 1/200$, $\theta = 1/3$, $Q = 2$.

parameters from Case 4 would fit the market prices for European call and put options exactly, then the leverage function would be identically equal to one and the SLV model reduces to the SV model. Clearly, Figure 3 indicates that the pure SV model with parameters from Case 4 doesn't match the market data very well. This outcome was to be expected, as the SV parameters from [2] do not correspond to a EUR/USD exchange rate.

With the obtained discrete leverage function, the performance of the calibration procedure is first tested by comparing the fully discrete approximations of the fair value of European call options which are acquired by numerically solving the systems of ODEs (4.4), (4.5), (5.1), (5.2). To this purpose we consider a range of strikes, given by

$$K = 0.7S_0, 0.8S_0, 0.9S_0, S_0, 1.1S_0, 1.2S_0, 1.3S_0.$$

Temporal discretization of (5.1) and (5.2) is performed by the classical *Crank–Nicolson scheme*. The systems (4.4) and (4.5), which are stemming from a two-dimensional PDE, are discretized in time by the MCS scheme (6.1) with parameter θ given above. For both methods we consider $\Delta\tau = 1/200$ and Rannacher time stepping is applied to handle the nonsmoothness of the initial functions. In Table 1 the obtained fully discrete approximations (FV_m), $m \in \{LVB, LVF, SLVB, SLVF\}$, of the fair value (FV) are presented in Case 1. Here $m = LVB$, respectively $m = LVF, SLVB, SLVF$, corresponds with the approximated fair value obtained via (5.1), respectively (5.2), (4.4), (4.5). In Table 1 one observes that the approximated option values are almost identical. To express in more detail the quality of the approximations, we present relative errors

$$\epsilon_{r,m} = (FV_m - FV_{LVB})/FV_{LVB}.$$

Here the option values given by solving (5.1), indicated by FV_{LVB} , are considered as the reference values. This is motivated by the fact that in practice one starts from the underlying LV model and within the LV model it is common to solve the backward equation (2.7). Table 1 reveals the favourable result that all relative errors are smaller than 0.1%. Numerical experiments for the other SV parameter sets, i.e. for Cases 2, 3, 4, yield the same observation. It can be concluded that the different approximations are almost identical in each of the four cases and the calibration procedure from Section 7 performs well.

When the strike increases relative to S_0 , the fair value of European call options tends to zero and it is difficult to adequately compare approximations. In financial practice, European call and put options are often quoted in terms of *implied volatility*. Let $\sigma_{imp,m}$ denote the implied volatility (in %) corresponding to FV_m . Figure 4 shows the implied volatilities obtained from

K/S_0	FV_{LVB}	FV_{LVF}	$\epsilon_{r,LVF}$	FV_{SLVB}	$\epsilon_{r,SLVB}$	FV_{SLVF}	$\epsilon_{r,SLVF}$
0.7	0.3288	0.3288	0.0000%	0.3288	0.0000%	0.3288	0.0000%
0.8	0.2228	0.2228	0.0000%	0.2228	0.0000%	0.2228	0.0001%
0.9	0.1185	0.1185	0.0008%	0.1185	0.0004%	0.1185	0.0008%
1	0.0381	0.0381	0.0083%	0.0381	0.0004%	0.0381	0.0079%
1.1	0.0091	0.0091	0.0235%	0.0091	0.0017%	0.0091	0.0211%
1.2	0.0019	0.0019	0.0437%	0.0019	0.0073%	0.0019	0.0391%
1.3	0.0004	0.0004	0.0661%	0.0004	0.0223%	0.0004	0.0640%

Table 1: Comparison of the approximated option values $FV_{LVB}, FV_{LVF}, FV_{SLVB}, FV_{SLVF}$ in Case 1 and for values $m_1 = 100, m_2 = 50, \Delta\tau = 1/200, \theta = 1/3, Q = 2$.

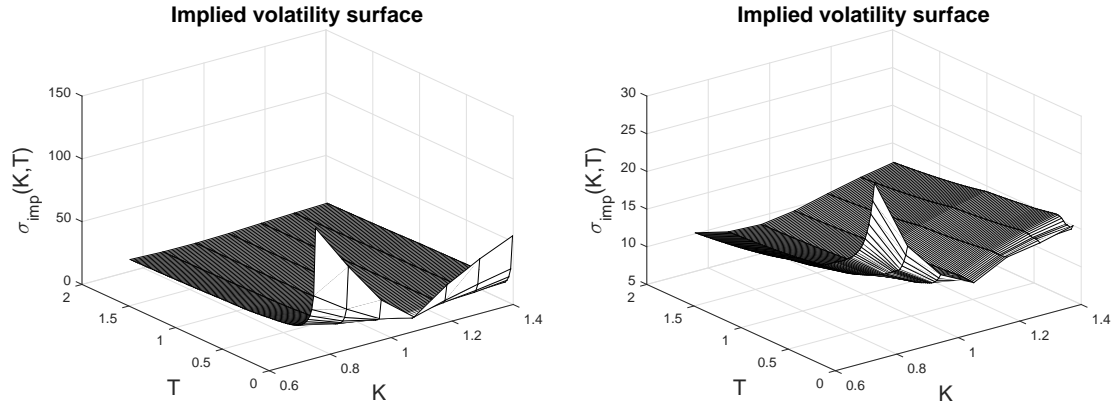


Figure 4: Implied volatilities obtained from the local volatility function from Figure 2 and FV_{LVF} with $m_1 = 100, \Delta t = 1/200$. The implied volatilities are shown approximately every week from $T = 1/200$ (left) and from $T = 1M$ (right).

the local volatility function from Figure 2 and FV_{LVF} with $m_1 = 100, \Delta t = 1/200$. The implied volatilities are shown approximately every week. In the following we test the performance of the calibration procedure by calculating the absolute implied volatility errors

$$\epsilon_m = |\sigma_{imp,m} - \sigma_{imp,LVB}|.$$

In Table 2 these errors are presented for the four different SV parameter sets, taking the same values of $m_1, m_2, \Delta\tau, \theta, Q$ as above. Since semidiscretization of (2.9) is performed by the adjoint spatial discretization, the only source of error in ϵ_{LVF} is the temporal discretization error. Table 2 shows that these errors are small. The somewhat larger values ϵ_{LVF} for $T = 6M$ compared to $T = 2Y$ can be explained from the fact that the implied volatility is more sensitive to changes in the fair value when the maturity is low. Table 2 subsequently reveals that in Case 1 and Case 3 the (small) errors ϵ_{SLVB} and ϵ_{SLVF} are of the same order of magnitude as ϵ_{LVF} . This indicates that the size of the error due to the calibration (with the iteration to handle the non-linearity) is not larger than the size of the temporal discretization error. As the calibration procedure includes numerical time stepping, this is the best result one can aim for. For Case 2 and Case 4 the magnitude of ϵ_{SLVB} is slightly higher than the one of ϵ_{LVF} . Additional numerical experiments reveal that this is closely related to a strongly violated Feller condition ($\frac{2\kappa\eta}{\xi^2} = 0.0296 \ll 1$). Probability mass is then stacked up near $v = 0$ and since our FD scheme is not positivity preserving, this sometimes leads to negative values for either the nominator or denominator of (7.2). In such situations, the calibration algorithm makes use of the conditional expectation of the previous time step, see Section 7, leading to a higher calibration error. Experiments with all parameter sets from [4,

Table 6.5] indicate that the calibration error is of the same order of magnitude as the temporal discretization error whenever $2\kappa\eta/\xi^2 \geq 0.15$. The worst results that we encountered were for parameter set I from [2] where a strongly violated Feller condition ($\frac{2\kappa\eta}{\xi^2} = 0.04$) is combined with a very high correlation ($\rho = -0.9$). Even for this extreme parameter set, however, the absolute implied volatility errors did not exceed 0.1.

In order to verify the assertions above, we repeat the numerical experiments with a smaller step size. In Table 3 the absolute implied volatility errors are given for the same parameters as above but where the calibration and pricing is performed with

$$\Delta\tau = 1/400.$$

Comparing ϵ_{LVF} in Tables 2 and 3, it is clearly seen that the temporal error decreases if $\Delta\tau$ decreases. Moreover, for Case 1 and Case 3, the absolute implied volatility errors $\epsilon_{SLVB}, \epsilon_{SLVF}$ are again of the same size as ϵ_{LVF} . For Case 2 and Case 4 the errors do not decrease equally fast. This can be seen as a consequence of the fact that the spatial discretization has not been changed and, hence, negative nominators and denominators of (7.2) are still observed. From additional experiments it can be concluded that, if the Feller condition is not strongly violated ($2\kappa\eta/\xi^2 \geq 0.15$), then for realistic values of $\Delta\tau$ the error introduced by the calibration procedure is of the same order of magnitude as the temporal discretization error. When the Feller condition is strongly violated, the calibration error is slightly higher.

Observe that by decreasing the step size, the reference values $\sigma_{imp,LVB}$ have slightly changed. This is a consequence of the fact that more points from the LV surface are used and the fully discrete solution FV_{LVB} converges to the semidiscrete solution $U_{LV,i_0}(T)$. We note that the approximated option values FV_{LVB} acquired with $\Delta\tau = 1/400$ are identical to those in Table 1 up to the number of digits presented in that table. This confirms again that the temporal discretization error is small.

As stated in Theorem 5.1, the condition (5.6) facilitates an exact match between the semidiscrete LV model and the semidiscrete SLV model whenever similar discretizations are used. This match is valid for any number of spatial grid points m_1, m_2 . In order to test this property of the calibration procedure, we repeat the numerical experiments with the number of spatial grid points replaced by

$$m_1 = 200, \quad m_2 = 100,$$

and with step size $\Delta\tau = 1/200$. The obtained implied volatilities σ_{LVB} are presented in Table 4 as well as the absolute implied volatility errors $\epsilon_{LVF}, \epsilon_{SLVB}, \epsilon_{SLVF}$.

One observes that the size of the ϵ_{LVF} is similar in Tables 2 and 4. Hence, the experiments indicate that the performance of the calibration procedure is independent of the number of spatial grid points. The difference between the approximations of the fair value by discretizing either (5.1), (5.2), (4.4) or (4.5) is always small.

By increasing m_1, m_2 the values $\sigma_{imp,LVB}$ have noticeably changed, which is related to the convergence of $U_{LV,i_0}(T)$ to the exact non-discounted fair value $u_{LV}(X_0, T)$. The differences in implied volatility in Tables 2, 3, 4 reveal that within the LV model and for the current, realistic values of m_1, m_2, τ the spatial discretization error is larger than the temporal discretization error (cf. Section 6). Since the calibration procedure from Section 7 matches the fully discrete LV and SLV models up to a difference with the size of the temporal discretization error, one can define an appropriate semidiscretization of the PDE (2.7), control the spatial discretization error within the LV model, and then calibrate the SLV model to the LV model such that the fully discrete SLV model matches the market data up to an error which is dominated by the controlled spatial error from semidiscretization within the LV model. If the Feller condition is strongly violated, one has to take into account a slightly higher calibration error.

We mention that all codes have been written in Matlab R2015a, where all matrices have been defined as sparse. The experiments have been performed on a computer with Intel Core i7-3540M 3.00GHz processor and 8GB memory. If the calibration is performed with $m_1 = 100, m_2 = 50, N = 100$ and $Q = 2$, then our implementation of the calibration procedure takes about 1 cpu-sec.

$T = 6M$			Case 1		Case 2	
K/S_0	$\sigma_{imp,LVB}$	ϵ_{LVF}	ϵ_{SLVB}	ϵ_{SLVF}	ϵ_{SLVB}	ϵ_{SLVF}
0.7	14.8646	0.0024	0.0024	0.0028	0.0008	0.0014
0.8	12.0458	0.0017	0.0015	0.0018	0.0004	0.0004
0.9	10.3061	0.0012	0.0006	0.0012	0.0057	0.0052
1	10.7970	0.0011	0.0000	0.0010	0.0006	0.0029
1.1	12.6393	0.0011	0.0001	0.0010	0.0176	0.0152
1.2	13.9656	0.0011	0.0002	0.0010	0.0260	0.0241
1.3	14.9511	0.0012	0.0004	0.0012	0.0094	0.0091

$T = 2Y$			Case 3		Case 4	
K/S_0	$\sigma_{imp,LVB}$	ϵ_{LVF}	ϵ_{SLVB}	ϵ_{SLVF}	ϵ_{SLVB}	ϵ_{SLVF}
0.7	10.2284	0.0008	0.0005	0.0008	0.0014	0.0012
0.8	9.1864	0.0005	0.0003	0.0005	0.0012	0.0011
0.9	8.9874	0.0004	0.0001	0.0004	0.0010	0.0011
1	9.6063	0.0004	0.0000	0.0004	0.0034	0.0036
1.1	10.6956	0.0004	0.0000	0.0004	0.0041	0.0044
1.2	11.6810	0.0004	0.0001	0.0004	0.0038	0.0040
1.3	12.4844	0.0004	0.0001	0.0004	0.0026	0.0026

Table 2: Comparison of the approximated implied volatilities $\sigma_{LVB}, \sigma_{LVF}, \sigma_{SLVB}, \sigma_{SLVF}$ for values $m_1 = 100, m_2 = 50, \Delta\tau = 1/200, \theta = 1/3, Q = 2$.

$T = 6M$			Case 1		Case 2	
K/S_0	$\sigma_{imp,LVB}$	ϵ_{LVF}	ϵ_{SLVB}	ϵ_{SLVF}	ϵ_{SLVB}	ϵ_{SLVF}
0.7	14.8605	0.0001	0.0007	0.0006	0.0004	0.0004
0.8	12.0438	0.0000	0.0002	0.0001	0.0003	0.0005
0.9	10.3053	0.0000	0.0000	0.0000	0.0016	0.0015
1	10.7964	0.0000	0.0000	0.0000	0.0046	0.0050
1.1	12.6386	0.0000	0.0000	0.0000	0.0002	0.0002
1.2	13.9647	0.0000	0.0001	0.0000	0.0066	0.0059
1.3	14.9498	0.0000	0.0001	0.0000	0.0006	0.0001

$T = 2Y$			Case 3		Case 4	
K/S_0	$\sigma_{imp,LVB}$	ϵ_{LVF}	ϵ_{SLVB}	ϵ_{SLVF}	ϵ_{SLVB}	ϵ_{SLVF}
0.7	10.2278	0.0001	0.0001	0.0001	0.0003	0.0003
0.8	9.1859	0.0000	0.0000	0.0000	0.0000	0.0000
0.9	8.9870	0.0000	0.0000	0.0000	0.0010	0.0011
1	9.6060	0.0000	0.0000	0.0000	0.0022	0.0022
1.1	10.6953	0.0000	0.0000	0.0000	0.0027	0.0027
1.2	11.6806	0.0000	0.0000	0.0000	0.0029	0.0028
1.3	12.4840	0.0000	0.0000	0.0000	0.0026	0.0026

Table 3: Comparison of the approximated implied volatilities $\sigma_{LVB}, \sigma_{LVF}, \sigma_{SLVB}, \sigma_{SLVF}$ for values $m_1 = 100, m_2 = 50, \Delta\tau = 1/400, \theta = 1/3, Q = 2$.

$T = 6M$			Case 1		Case 2	
K/S_0	$\sigma_{imp,LVB}$	ϵ_{LVF}	ϵ_{SLVB}	ϵ_{SLVF}	ϵ_{SLVB}	ϵ_{SLVF}
0.7	14.6017	0.0032	0.0039	0.0042	0.0028	0.0033
0.8	11.9199	0.0020	0.0019	0.0021	0.0006	0.0005
0.9	10.2664	0.0013	0.0006	0.0013	0.0052	0.0048
1	10.8100	0.0011	0.0001	0.0010	0.0022	0.0043
1.1	12.6442	0.0011	0.0001	0.0010	0.0134	0.0111
1.2	13.9412	0.0012	0.0002	0.0010	0.0294	0.0276
1.3	14.8890	0.0012	0.0004	0.0011	0.0102	0.0100

$T = 2Y$			Case 3		Case 4	
K/S_0	$\sigma_{imp,LVB}$	ϵ_{LVF}	ϵ_{SLVB}	ϵ_{SLVF}	ϵ_{SLVB}	ϵ_{SLVF}
0.7	10.1742	0.0009	0.0006	0.0010	0.0011	0.0009
0.8	9.1690	0.0006	0.0003	0.0006	0.0010	0.0009
0.9	8.9858	0.0004	0.0001	0.0004	0.0013	0.0014
1	9.6089	0.0004	0.0000	0.0004	0.0039	0.0041
1.1	10.6981	0.0004	0.0000	0.0004	0.0047	0.0050
1.2	11.6825	0.0004	0.0001	0.0004	0.0045	0.0047
1.3	12.4837	0.0004	0.0001	0.0004	0.0033	0.0034

Table 4: Comparison of the approximated implied volatilities $\sigma_{LVB}, \sigma_{LVF}, \sigma_{SLVB}, \sigma_{SLVF}$ for values $m_1 = 200, m_2 = 100, \Delta\tau = 1/200, \theta = 1/3, Q = 2$.

Note that the computing time is (approximately) directly proportional to the number of spatial grid points $m = m_1 m_2$, the number of time steps N , and the number of iterations Q .

9 Conclusion

In financial practice, SLV models are calibrated to market data for European call and put options by calibrating them to their underlying LV models. Since there is often no closed-form analytical formula available for the fair value of vanilla options under an LV model, the best one can aim for is that the approximations of the fair value given by the two models are identical whenever similar numerical valuation methods are used. Here, we choose to perform the numerical option valuation by semidiscretizing the respective backward Kolmogorov equations with finite differences. By making use of an adjoint semidiscretization of the corresponding forward Kolmogorov equations, we derived an expression for the leverage function such that the semidiscretized SLV model is calibrated exactly to the semidiscretized LV model. In order to employ this expression, one has to solve a large non-linear system of ODEs. For the actual numerical calibration, temporal discretization of this system by a suitable ADI method is combined with an inner iteration to deal with the non-linearity. Our numerical experiments reveal that the fully discrete approximations of the fair value of European call options under the LV and SLV models are the same up to the size of the temporal discretization error. Since the spatial discretization error is typically much larger than the temporal discretization error, one can control the former one by defining an appropriate semidiscretization of the LV model and then calibrate the fully discrete SLV model de facto exactly to the fully discrete LV model. Only if the Feller condition is strongly violated, one has to take into account a slightly higher calibration error.

Acknowledgements

The authors gratefully acknowledge Sven Foulon and an anonymous reviewer for their valuable comments on the topic of this paper. The work by the first author has been supported financially

by a PhD Fellowship of the Research Foundation–Flanders.

References

- [1] ANDERSEN, L. B. G., PITERBARG, V. V. (2007) Moment explosions in stochastic volatility models. *Finance Stoch.*, **11**, 29–50.
- [2] ANDERSEN, L. B. G. (2008) Simple and efficient simulation of the Heston stochastic volatility model. *J. Comp. Finan.*, **11**, 1–42.
- [3] ANDREASEN, J., HUGE, B. (2011) Volatility interpolation. *Risk*, March, 76–79.
- [4] CLARK, I. J. (2011) *Foreign Exchange Option Pricing: A Practitioner’s Guide*. John Wiley & Sons.
- [5] CRAIG, I. J. D., SNEYD, A. D. (1988) An alternating-direction implicit scheme for parabolic equations with mixed derivatives. *Comp. Math. Appl.*, **16**, 341–350.
- [6] DUPIRE, B. (1994) Pricing with a smile. *Risk*, January, 18–20.
- [7] EKSTRÖM, E., TYSK, J. (2011) Boundary conditions for the single-factor term structure equation. *Ann. Appl. Prob.*, **21**, 332–350.
- [8] ENGELMANN, B., KOSTER, F., OELTZ, D. (2012) Calibration of the Heston stochastic local volatility model: a finite volume scheme. *Available at SSRN 1823769*.
- [9] GYÖNGY, I. (1986) Mimicking the one-dimensional marginal distributions of processes having an Ito differential. *Probab. Th. Rel. Fields*, **71**, 501–516.
- [10] HAENTJENS, T., IN ’T HOUT, K. J. (2012) Alternating direction implicit finite difference schemes for the Heston–Hull–White partial differential equation. *J. Comp. Finan.*, **16**, 83–110.
- [11] HENRY-LABORDÈRE, P. (2009) Calibration of local stochastic volatility models to market smiles. *Risk*, September, 112–117.
- [12] IN ’T HOUT, K. J., FOULON, S. (2010) ADI finite difference schemes for option pricing in the Heston model with correlation. *Int. J. Numer. Anal. Mod.*, **7**, 303–320.
- [13] IN ’T HOUT, K. J., MISHRA, C. (2011) Stability of the modified Craig–Sneyd scheme for two-dimensional convection-diffusion equations with mixed derivative term. *Math. Comp. Simul.*, **81**, 2540–2548.
- [14] IN ’T HOUT, K. J., MISHRA, C. (2013) Stability of ADI schemes for multidimensional diffusion equations with mixed derivative terms. *Appl. Numer. Math.*, **74**, 83–94.
- [15] IN ’T HOUT, K. J., WELFERT, B. D. (2009) Unconditional stability of second-order ADI schemes applied to multi-dimensional diffusion equations with mixed derivative terms. *Appl. Numer. Math.*, **59**, 677–692.
- [16] IN ’T HOUT, K. J., WYNS, M. (2016) Convergence of the Modified Craig–Sneyd scheme for two-dimensional convection-diffusion equations with mixed derivative term. *J. Comp. Appl. Math.*, **296**, 170–180.
- [17] HUNSDORFER, W., VERWER, J. G. (2003) *Numerical Solution of Time-Dependent Advection-Diffusion-Reaction Equations*. Berlin: Springer.
- [18] ITKIN, A. (2015) High-order splitting methods for forward PDEs and PIDEs. *Int. J. Theor. Appl. Finance*, **18**, 1550031-1 – 1550031-24.

- [19] ITKIN, A. (2017) Modeling stochastic skew of FX options using SLV models with stochastic spot/vol correlation and correlated jumps. *Available at* <https://arxiv.org/abs/1701.02821>.
- [20] LIPTON, A. (2001) *Mathematical Methods for Foreign Exchange: A Financial Engineer's Approach* Singapore: World Scientific.
- [21] LIPTON, A. (2002) The vol smile problem. *Risk*, February, 61–65.
- [22] MISHRA, C. (2014) *Stability of Alternating Direction Implicit Schemes with Application to Financial Option Pricing Equations*. PhD thesis, University of Antwerp.
- [23] POOLEY, D. M., VETZAL, K. R., FORSYTH, P. A. (2003) Convergence remedies for non-smooth payoffs in option pricing. *J. Comp. Finan.*, **6**, 25–40.
- [24] RANNACHER, R. (1984) Finite element solution of diffusion problems with irregular data. *Numer. Math.*, **43**, 309–327.
- [25] REN, Y., MADAN, D., QIAN, M. Q. (2007) Calibrating and pricing with embedded local volatility models. *Risk*, September, 138–143.
- [26] RISKEN, H. (1989) *The Fokker-Planck Equation: Methods of Solution and Applications*, 2nd edition. Berlin: Springer.
- [27] SCOTT, L. O. (1987) Option pricing when the variance changes randomly: theory, estimation, and an application. *J. Financ. Quant. Anal.*, **22**, 419–438.
- [28] TACHET, R. (2011) *Non-parametric model calibration in finance*. PhD thesis, Ecole Centrale Paris.
- [29] TATARU, G., FISHER, T. (2010) Stochastic Local Volatility. *Technical report, Quantitative Development Group, Bloomberg*.
- [30] TAVELLA, D., RANDALL, C. (2000) *Pricing Financial Instruments: The Finite Difference Method*. New York: John Wiley & Sons.
- [31] VAN DER STOEP, A. W., GRZELAK, L. A., OOSTERLEE, C. W. (2014) The Heston Stochastic-Local Volatility Model: Efficient Monte Carlo Simulation. *Int. J. Theor. Appl. Finan.*, **17**, 1450045-1–1450045-30.
- [32] WYNS, M. (2016) Convergence analysis of the Modified Craig–Sneyd scheme for two-dimensional convection-diffusion equations with nonsmooth initial data. To appear in *IMA J. Numer. Anal.*, <http://dx.doi.org/10.1093/imanum/drw028>.